

# Source characteristics of the 1989 Boca del Tocuyo earthquakes in northwestern Venezuela

Gustavo Malavé<sup>1</sup> and G. Suárez<sup>2,\*</sup>

<sup>1</sup> *Fundación Venezolana de Investigaciones Sismológicas, Caracas, Venezuela*

<sup>2</sup> *Instituto de Geofísica, Universidad Nacional Autónoma de México, Mexico City, México.*

Received: March 16, 2007; accepted: August 14, 2007

## Resumen

El sismo de Boca del Tocuyo del 30 de abril de 1989 tiene un significado especial en la evaluación del peligro sísmico del norte de Venezuela y en la comprensión de la compleja deformación tectónica que tiene lugar en esta zona. A pesar de que se trata de un sismo de magnitud moderada ( $M_w=6.2$ ), el evento principal y su réplica mas grande ( $M_w=5.6$ ) produjeron daños considerables en estructuras de baja altura, principalmente debido a fallamiento del suelo y a la intensa licuefacción que fue provocada por el sismo en las localidades costeras cercanas a la zona epicentral. Ambos sismos muestran un tren de ondas de volumen que son mucho más largas que las que se esperarían para eventos de esa magnitud. La razón de esta duración anómalamente larga fue analizada por medio de la inversión formal de las ondas P, SH y SV que fueron registradas a distancias teleseísmicas. Los resultados muestran que el evento principal de Boca del Tocuyo fue generado por un complejo proceso de ruptura compuesto por al menos dos y tal vez tres sub-eventos, mientras que la réplica más grande está formada por dos sub-eventos. A pesar de que la dirección de propagación de la ruptura no pudo ser determinada directamente de los datos teleseísmicos de ondas de volumen, la relocalización epicentral de la réplica mayor, la distribución de cerca de 60 réplicas ( $m_b<4.5$ ), así como la linealidad de la costa, que es paralela a las estructuras geológicas de esta zona, sugieren un movimiento lateral derecho sobre una falla transcurrente orientada en dirección NO-SE. Los sismos de Boca del Tocuyo fueron aparentemente generados en un sistema de fallas que son oblicuos a la dirección preferencial este-oeste que guardan las grandes fallas que definen las fronteras de placa en el norte de Venezuela.

**Palabras clave:** Tectónica del Caribe, peligro sísmico, ruptura compleja de una falla sísmica.

## Abstract

The Boca del Tocuyo earthquake of April 30, 1989, has a special significance in assessing the seismic hazard of northern Venezuela and in understanding the complex tectonic deformation in this area. Although it was an event of moderate magnitude ( $M_w=6.2$ ), the mainshock and its largest aftershock ( $M_w=5.6$ ) produced considerable damage in low-rise structures, mainly due to soil failure, and induced intense liquefaction in most of the coastal towns near the epicentral area. Both earthquakes show body-wave trains which are much longer than those expected for events of such magnitude. The reason for this anomalous duration was analyzed through the formal inversion of the P, SH, and SV waves recorded teleseismically. The results show that the Boca del Tocuyo main event was generated by multiple rupture processes composed of at least two and perhaps three subevents, whereas the aftershock was formed by two subevents. Although the direction of rupture propagation could not be gleaned directly from the teleseismic body wave data, the epicentral relocation of the largest aftershock, the hypocentral distribution of about 60 aftershocks ( $m_b<4.5$ ), and the linearity of the coast, which is parallel to the geologic structures in this area, suggest right-lateral, strike-slip faulting in a NW-SE direction. The Boca del Tocuyo earthquakes were apparently generated on a system of conjugate faults that are oblique to the east-west-trending, major fault systems that define the plate boundaries in northern Venezuela.

**Key words:** Venezuela, Caribbean tectonics, seismic hazard, complex seismic rupture.

## Introduction

On April 30, 1989, Boca del Tocuyo and several neighbouring coastal towns in north-western Venezuela were severely damaged by a moderate-sized earthquake ( $m_b=5.7$ ;  $M_s=6.0$ ) (Figure 1). This is the largest earthquake in central and western Venezuela since the magnitude 6.6 ( $M_w$ ) Caracas event occurred on July 30, 1967. Four days later, on May 4, 1989, the largest aftershock ( $m_b=5.4$ ;

$M_s=5.2$ ) took place (Table 1). This aftershock caused concern among the inhabitants of this region and lightly damaged several low-rise dwellings.

The epicentral area of the Boca del Tocuyo seismic sequence lies close to the zone where the Oca-Ancón, Boconó, and Morón fault systems converge (Figure 1). These fault systems have been proposed as the border between the Caribbean and South American plates in

Table 1

Focal Parameters of the Boca del Tocuyo Earthquake and its Largest Aftershock

Event	Source	Lat °N	Lon °W	Depth km	$m_b$	Strike deg	Dip deg	Slip deg	$M_0$ $10^{18}$ Nm
Apr. 30, 1989	ISC	10.99	68.31	20.0	5.7	--	--	--	--
	NEIC	10.96	68.33	20.0	5.9	242	36	147	0.81
	FUNVISIS	11.10	68.18	11.1	5.7	75	45	-149	--
	CMTS	10.88	68.08	15.0	--	166	62	-168	0.98
	<i>This study</i>	11.01	68.25	14.0*	--	162*	82*	-177*	3.50*
May 4, 1989	ISC	11.07	68.26	10.0	5.4	--	--	--	--
	NEIC	11.04	68.27	16.0	5.4	--	--	--	--
	FUNVISIS	11.14	68.21	13.6	5.0	75	45	-149	--
	CMTS	10.96	68.42	15.0	--	145	51	-174	0.21
	<i>This study</i>	11.06	68.23	12.0*	--	130*	90*	-172*	0.24*
	JHD89	10.98	68.34	17.4	--	--	--	--	--

CMTS: Centroidal moment tensor solution (Dziewonski *et al.*, 1990).

\* Best double-couple of the moment tensor sum of the subevents. Parameters of the subevents are resumed on Table 4.

western Venezuela (e.g., Molnar and Sykes, 1969; Soulas, 1986). However, the present rates of motion of the Oca-Ancón fault system (2.5-4.0 mm/yr) (Soulas *et al.*, 1987) and of the Boconó fault system (0.3 cm/yr-1.4 cm/yr) (e.g., Schubert, 1982; Soulas, 1986) are lower than the predicted relative velocity between the Caribbean and South American plates ( $\sim 2$  cm/yr) proposed from kinematics plate motions (Jordan, 1975; Minster and Jordan, 1978; Stein *et al.*, 1988; Sykes *et al.*, 1982). Thus the relative motion between the Caribbean and South American plates is apparently not absorbed on a single fault. This motion appears to be distributed over a wide zone of deformation along major right-lateral, strike-slip fault systems (e.g., Soulas, 1986) (Figure 1).

Besides these major fault systems, several conjugate faults near the epicentral area of the Boca del Tocuyo earthquakes appear to be seismically capable (Soulas, 1986). These faults are oriented mainly in a NW-SE direction and they have been identified at sea, where they appear to cut the seafloor (Barbot *et al.*, 1979; Barbot *et al.*, 1980) (Figure 1). As discussed later, this fault system apparently controls the orientation of the coastline in this area and presumably one of them ruptured during the Boca del Tocuyo seismic sequence.

The Boca del Tocuyo earthquake and its largest aftershock show several interesting aspects. The focal mechanisms reported by Dziewonski *et al.* (1990), the National Earthquake Information Center (NEIC) (Sipkin,

1991), and FUNVISIS (Venezuelan Seismological Research Foundation) show important differences (Figure 2). The mechanisms determined by Dziewonski *et al.* (1990) show a mostly strike-slip faulting mechanism. On the other hand the focal mechanism determined by FUNVISIS, based on the sparse local data, indicate normal faulting on NW-SE planes, whereas the fault plane solution suggested by Sipkin (1991) indicates reverse faulting on NW-SE nodal planes (Figure 2). These striking differences in the source mechanisms proposed by various authors underline the importance of obtaining an independent and reliable fault plane solution, which in turn may be compared with the active faults mapped in the area.

The 1989 Boca del Tocuyo earthquakes are the only events reported in this region during both historical and instrumental seismological periods (Singer *et al.*, 1992). Furthermore, both earthquakes induced intense liquefaction in an area located  $\sim 25$  km away from the epicenter. According to the relations proposed by Ambraseys (1988) ( $M_w$  vs. distance from the epicenter to the site liquefied), events of this magnitude are capable of causing the observed liquefaction. However, this phenomenon was particularly strong and widespread in Boca del Tocuyo due to the local soil conditions. Here we explore whether the source characteristics of the main event contributed to the observed intense liquefaction.

In this study, the epicentral locations of the Boca del Tocuyo earthquake and its largest aftershock were

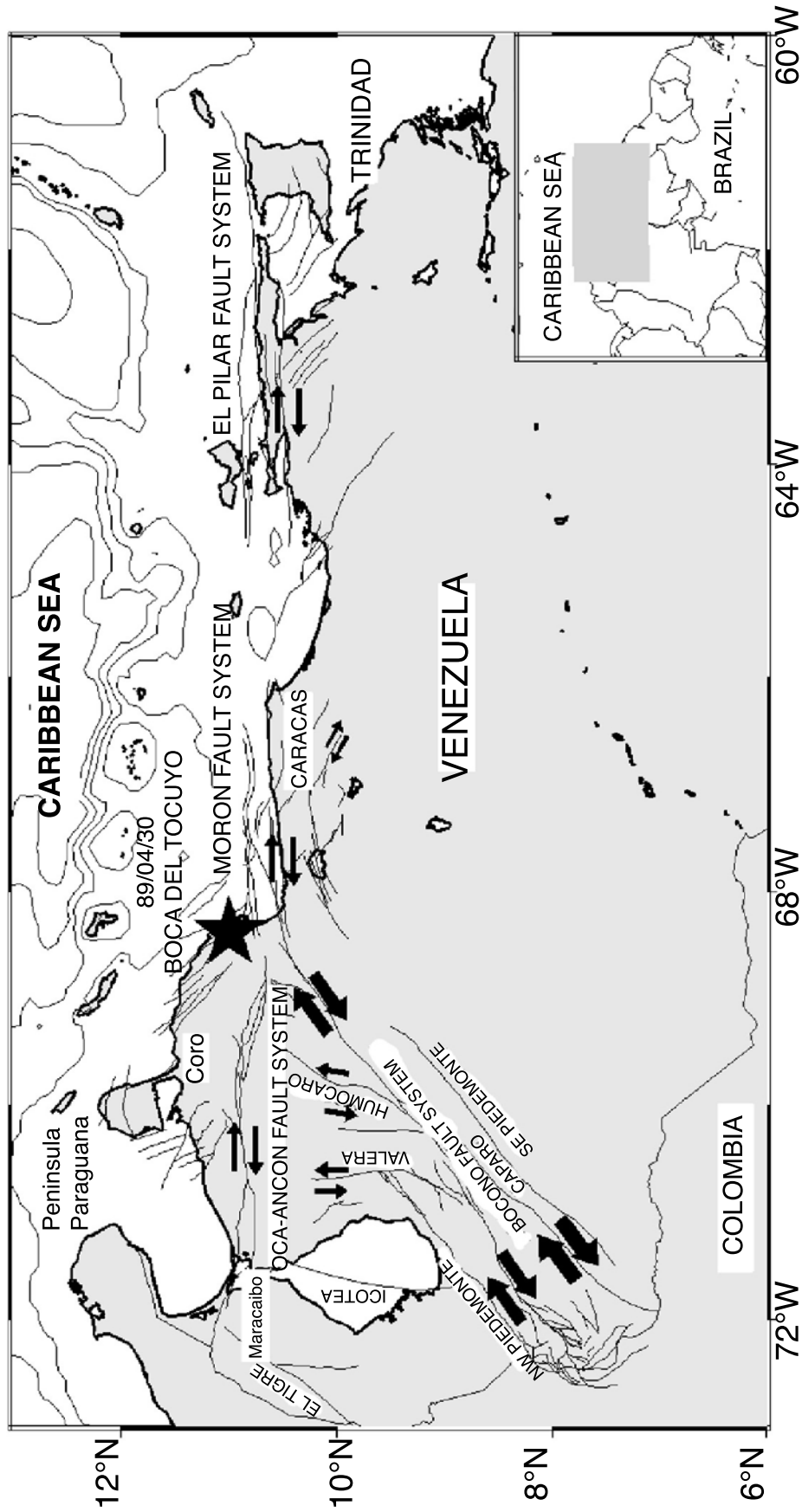


Fig. 1. Major active fault systems in northern Venezuela (after Singer *et al.*, 1992; Soulas, 1986; Soulas *et al.*, 1987). The star shows the epicentral location of the Boca del Tucuyo seismic sequence, where a maximum intensity of VII (MMI) was assigned by De Santis *et al.* (1991). The opposing arrows indicate the relative motion of the faults. Bathymetry is in meters.

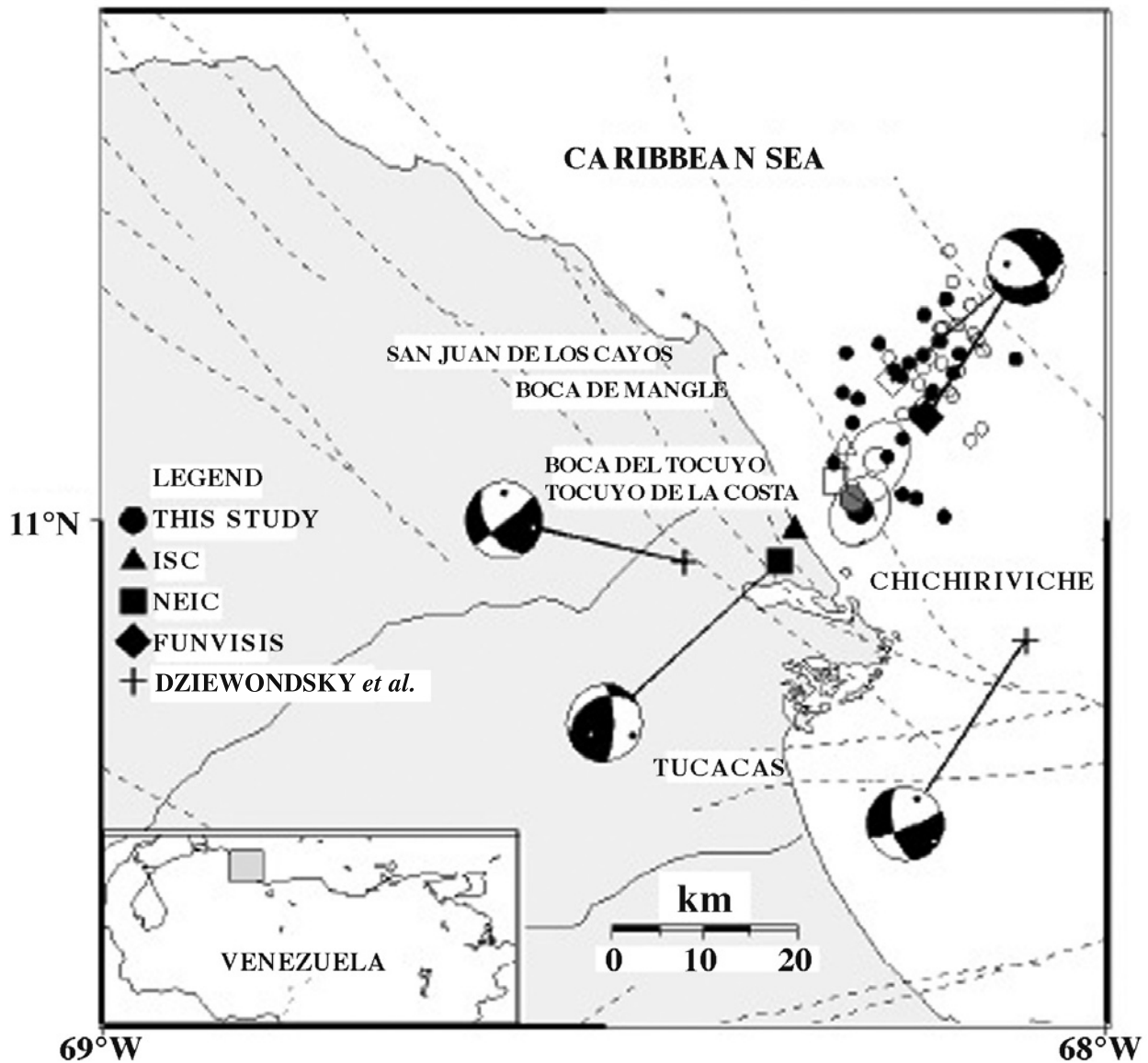


Fig. 2. Epicentral locations determined by the ISC (triangles), NEIC (squares), FUNVISIS (diamonds), Dzierowski *et al.* (1990) (crosses), and this study (large circles) for the Boca del Tocuyo events. The main shock is represented as a solid symbol and the largest aftershock as the corresponding open symbols. In the case of Dzierowski *et al.* (1990) solutions, the mainshock was located offshore. The uncertainties in the epicentral locations determined in this study (large closed and open circles respectively) are shown as 90% confidence ellipses. The hatched large circle indicates the relocation of the largest aftershock using the JHD method of Dewey (1971). The small circles represent the epicenters of the aftershocks located by Singer *et al.* (1992) ( $m_b < 4.5$ ); depths ranging from 0 to 9 km (open circles) and from 10 to 24 km (solid circles). The black quadrants in the focal mechanisms indicate compressional arrivals projected in a lower hemisphere projection. The open and solid circles in the mechanisms correspond to the position of the T and P axes on the focal sphere, respectively.

The dashed lines are active fault traces (Singer *et al.*, 1992). Solid lines at sea are bathymetric curves in meters.

evaluated. Furthermore, a detailed analysis of the long-period body waves using a formal least squares inversion algorithm (Nábelek, 1984) was carried out for both events in order to characterize their time history and the rupture process. The results suggest that the Boca del Tocuyo events originated from unusually complex and long rupture processes for earthquake of that magnitude.

### Epicentral Location and Intensity Distribution

#### *Epicentral Location of the Mainshock and of the Largest Aftershock*

The epicentral locations of the main event and its largest aftershock were determined with the program SE89

(Dewey, 1971), using the information collected from the Earthquake Data Report (*EDR*) of the *NEIC* (355 and 256 stations for the mainshock and aftershock respectively), and the 1968 seismological travel-time tables (Herrin *et al.*, 1968). In the calculation of those locations with the single-event method, arrival times showing large errors (residuals greater than 2 s) were eliminated in order to have a better quality control over the stations included in the database. After the last iteration, the number of stations in the database was reduced to 249 and 232 for the mainshock and aftershock, respectively.

There are some differences between these locations and those reported by the International Seismological Centre (*ISC*), *NEIC*, and *FUNVISIS* (Table 1). The epicentral locations of the mainshock reported by *ISC* and *NEIC* are on land, near the most severely damaged towns, whereas the locations reported by *FUNVISIS* and that determined in this study lie offshore, 15.5 km and 4.5 km away from the coast respectively (Figure 2). On the other hand, the epicenters of the largest aftershock calculated by *ISC* and *NEIC* lie, on average, 5.5 km away from the coast and are very close to the mainshock epicentral location determined in this study (Figure 2). *FUNVISIS* used in their hypocentral estimations only local seismological stations distributed to the south of the epicenter and thus it is not surprising that their epicenter is "pulled" south towards the network. In the determination of the epicentral locations in this study, besides the local stations used for *FUNVISIS*, many other regional and teleseismic stations were included to complete a good azimuthal coverage. The location proposed in this paper benefits from the fact that local, regional and teleseismic data are used to recompute the epicentres. The differences between the location obtained in this study and those of *NEIC* and the *ISC* are within the errors normally observed for teleseismic locations.

The largest aftershock was relocated with respect to the epicenter of the mainshock calculated in this study, using the Joint Hypocenter Determination (*JHD*) method (Dewey, 1971). The relocated epicenter of the largest aftershock lies two km to the NW of the mainshock (Figure 2). However, no conclusive evidence may be drawn about the fault orientation based only on the location of the largest aftershock. An attempt to relocate also a foreshock ( $m_b=4.9$ ) and two other smaller aftershocks ( $m_b=4.6$ ) was unsuccessful because they were not big enough to be detected by an adequate number of stations, resulting in epicenter locations with large 90% confidence ellipses.

#### *Intensity Distribution*

The intensity information collected by De Santis *et al.* (1991) shows a maximum value of VII Modified Mercalli Intensity (MMI) near the towns of Boca del Tocuyo, Tocuyo

de la Costa, Chichiriviche, Boca del Mangle, and San Juan de los Cayos (Figure 2). Most of the damage observed corresponds to fissures or to the collapse of walls in houses of defective masonry, and tilting of houses and water-tanks due to soil failure (De Santis *et al.*, 1991; Audemard and De Santis, 1991).

Both the main event and the largest aftershock induced liquefaction in the coastal area close to the epicenters. Isolated and aligned sand-boils, and vent-fractures were observed within a radius of about 25 km from the epicentral region. The most spectacular liquefaction features occurred in the town of Boca del Tocuyo. There, the volume of water ejected inundated a zone of approximately 5000 m<sup>2</sup> with a water layer of 10 to 15 cm. The fact that the largest aftershock also induced liquefaction is demonstrated by the presence of overlapped sand-boils, where younger sand-boils cut older ones. No strong motion records are available in the near field and the accelerations estimated from empirical correlation and field observations are in the range of 0.25-0.30 g (De Santis *et al.*, 1991). Based on empirical relations between MMI values and acceleration, Malaver (1990) estimated a maximum average acceleration of 0.38 g where liquefaction took place, and a value of 0.09 g outside this region.

### **Inversion of Body Waves**

#### *Data Preparation and Inversion Method*

The source parameters of the Boca del Tocuyo earthquake and its largest aftershock were analyzed through the inversion of long-period *P*, *SH*, and *SV* waves recorded by the Global Digital Seismograph Network (*GDSN*). Only seismograms of stations within an epicentral distance range of 27° to 90° were included in the study. All seismograms were high-pass filtered with a cut-off period of 60 s in order to remove long-period noise. The crustal structure in the source region and below the recording stations was assumed to be a half-space with a compressional wave velocity of 6 km/s, a Poisson ratio of 0.25, and a density of 2.75 g/cm<sup>3</sup>. The anelastic attenuation along the propagation path was parameterized using a  $t^*=1$  s for *P* waves, and a  $t^*=4$  s for *SH* and *SV* waves.

The inversion procedure is discussed in detail by Nábelek (1984). According to the size and complexity of the earthquake, the source time function is parameterized as a single point source or as an event composed of several point sources (subevents) separated in time and space. For each subevent, the model parameters include the fault plane solution (strike, dip, and rake), centroidal depth, seismic moment, source time function, and the relative location and time delay of each subevent with respect to the first one. The source time function is allowed to take an arbitrary shape.

Theoretical seismograms are iteratively matched to the observed seismograms using a least squares criterion until a prescribed variance reduction is achieved. The seismic phases and stations used in the inversion procedure are shown on Tables 2 and 3.

*Inversion Strategy*

The observed waveforms strongly suggest that the Boca del Tocuyo mainshock and largest aftershock were complex events. The duration of the body wave trains was about 75 s. This duration is, on average, twice as long as that expected for an earthquake of this magnitude. As a first step, the two events were analyzed assuming a single point source with a source time function duration of about four seconds. This source time function corresponds approximately to the duration of a single event of that magnitude. In both cases, the starting source mechanism for the inversion was the centroidal moment tensor solution (Dziewonski *et al.*, 1990) (Table 1; Figure 2). Attempts to use the NEIC fault plane solution (Sipkin, 1991) as the initial source mechanism proved unsuccessful.

Assuming a single point source, only the initial part of the waveforms could be modeled. Thus in order to synthesize the longer body-wave trains, we first investigated the possibility that the long duration was caused by local reverberation of body waves in the upper crust. Because the velocity structure of the Boca del Tocuyo region is not well known, a realistic velocity model of neighbouring zones with similar conditions was used. Therefore, several inversions were attempted using the velocity model reported by Gajardo *et al.* (1986) for the

east coast of Lake Maracaibo. To this velocity structure, low-velocity layers with high impedance contrasts were added in the upper crust.

The various source models including these low-velocity layers were tested as follows. First, a two-km-thick, low-velocity layer with a *P*-wave velocity ratio ( $V_1/V_2$ ) of 2.9/6.0 km/s was added in the upper crust. Next, a second velocity model was prescribed where a low-velocity layer with a thickness of 3 km and with a *P*-wave velocity ratio ( $V_1/V_2$ ) of 6.0/4.2 km/s was included in the upper crust, and a second low-velocity layer with a *P*-wave velocity ratio ( $V_2/V_3$ ) of 4.2/8.2 km/s was placed above the Moho. All these attempts, however, were unsuccessful to reproduce the complexity and long duration of the observed waveforms.

There are several cases of moderate-sized earthquakes that have generated complex *P* waves, but very simple *SH* waveforms. Two examples are: the two aftershocks located north of Atka Island that occurred after the Andreanof Island earthquake of May 7, 1986 (Boyd and Nábelek, 1988), and the two events of January 10, 1979, that occurred in the Makran region (Byrne *et al.*, 1992). In both cases, because of the similarity of the *P* waveforms for each pair of events, and taking into account the simplicity of the *SH* waves, the authors concluded that the complexities in the *P* waveforms were caused by near-source, crustal structure effects rather than by a complex source process. Boyd and Nábelek (1988), however, were unable to duplicate the waveforms adding low-velocity layers and a high-contrast layer above the Moho to the velocity structure. Byrne *et al.* (1992), on the other hand, were able to improve the fit of the waveforms adding a low-velocity zone to their prescribed velocity model.

**Table 2**

Seismic Stations Used in the Inversion of Boca del Tocuyo Mainshock

Station	Azimuth deg	Epicentral Distance °	Wave Type	Network
KEV	20.5	81.7	P, SH	DWWSSN
KONO	31.0	74.5	P, SV, SH	ASRO
GRFO	41.4	75.0	P, SV, SH	SRO
TOL	50.9	63.3	P, SV, SH	DWWSSN
BCAO	86.3	86.1	P, SV, SH	SRO
ZOBO	179.6	27.1	P, SH	ASRO
ANMO	310.8	42.1	SV, SH	SRO
LON	319.0	57.4	P, SV, SH	DWWSSN
COL	334.4	75.7	P	DWWSSN
SCP	345.8	30.9	P, SV, SH	DWWSSN
GAC	351.3	35.2	P, SV, SH	SRO

**Table 3**

Seismic Stations Used in the Inversion of Boca del Tocuyo Aftershock

Station	Azimuth deg	Epicentral Distance °	Wave Type	Network
KONO	31.0	74.4	SH	ASRO
GRFO	41.4	74.9	SH	SRO
ANTO	49.1	91.3	SH	SRO
BCAO	86.3	86.0	SH	SRO
ZOBO	179.7	27.1	P	ASRO
ANMO	310.7	42.1	P, SH	SRO
LON	319.0	57.4	SH	DWWSSN
SCP	345.7	30.8	P	DWWSSN
GAC	351.3	35.2	P, SH	SRO

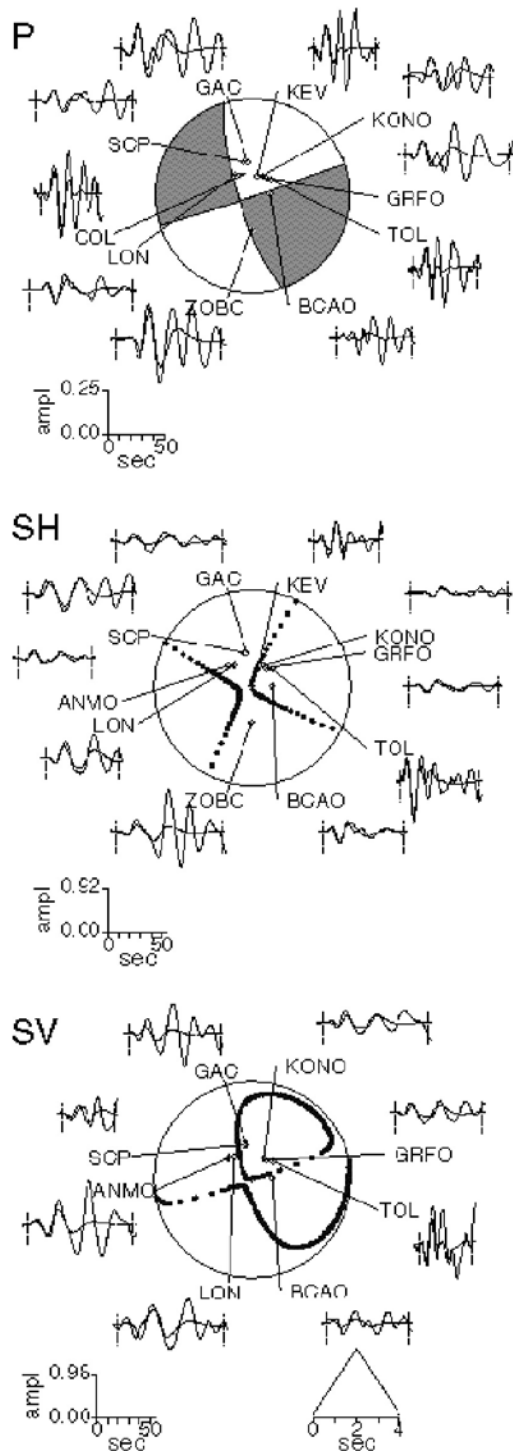


Fig. 3. Results of the simultaneous inversion of the long-period (top) P, (middle) SH, and (bottom) SV waves of the Boca del Tocuyo mainshock using a single point source with a source time function duration of 4 s. The theoretical seismograms (dashed lines) match well only the first part of the observed waveforms (solid lines) at all the stations. The focal mechanisms are shown in a lower hemisphere projection. The hatched areas in the P waves fault plane solution represent compressional first motion. Amplitudes of the waveforms are normalized to an instrumental magnification of 1500 and a geometrical spreading corresponding to an epicentral distance of 40°.

It is worth stressing that contrary to the examples mentioned above, the Boca del Tocuyo earthquakes show an anomalously long duration and complexity not only in the *P* waveforms, but also on the *SH* and *SV* signals. Thus it is more likely that the complexity of these waveforms is the result of a multiple rupture process than due to the local structure.

#### A Multiple Rupture Process

The source model of the Boca del Tocuyo events was obtained following a similar inversion strategy to that used by Suárez and Nábelek (1990) for the Caracas earthquake of July 30, 1967. First, it was assumed that the main event was caused by a single point source with a long source time function duration of 30 s. The inversion resulted in the average (centroidal) mechanisms indicated on Table 4. The resulting source time function shows that it is composed of three main subevents spaced in time (Figure 4). A single point source with a long source time function defines the same focal mechanism for all subevents. Although the fit of the synthetic waveforms is not yet satisfactory, the resulting three subevents of the mainshock approximately match most of the observed seismograms for about 50 seconds (Figure 4). A similar conclusion is reached in the case of the largest aftershock, where at least two subevents are needed to model the waveforms.

As a second step, each of the three subevents that resulted from the previous inversion using a single, long source time function was analyzed independently by freeing the parameters related only to a particular subevent. For example, in the case of the first subevent, the time series were inverted within a time frame that included only that particular subevent. After an adequate fit was obtained for this first subevent, the inversion was applied to the time frame corresponding to the second subevent, and finally to the time window of the third one. Once this stepwise inversion of the waveforms was completed, all parameters were freed and the inversion was allowed to iterate freely to the best fitting solution using the complete waveforms (Figures 5 and 6). The final results showing the parameters of the subevents of both earthquakes are summarized on Table 4.

In the case of the mainshock, the second and third subevents triggered 12.4 s and 27.6 s after the origin time. The depths of the subevents decrease from 17.5 km for the first one to 10.8 km for the last. The total seismic moment release (tensor sum) of the mainshock is  $2.4 \times 10^{18}$  Nm, which corresponds to a moment magnitude  $M_w = 6.2$  (Hanks and Kanamori, 1979). The three subevents composing the mainshock indicate a strike-slip faulting mechanism (Figure 5). Subevents 1 and 3 are the best

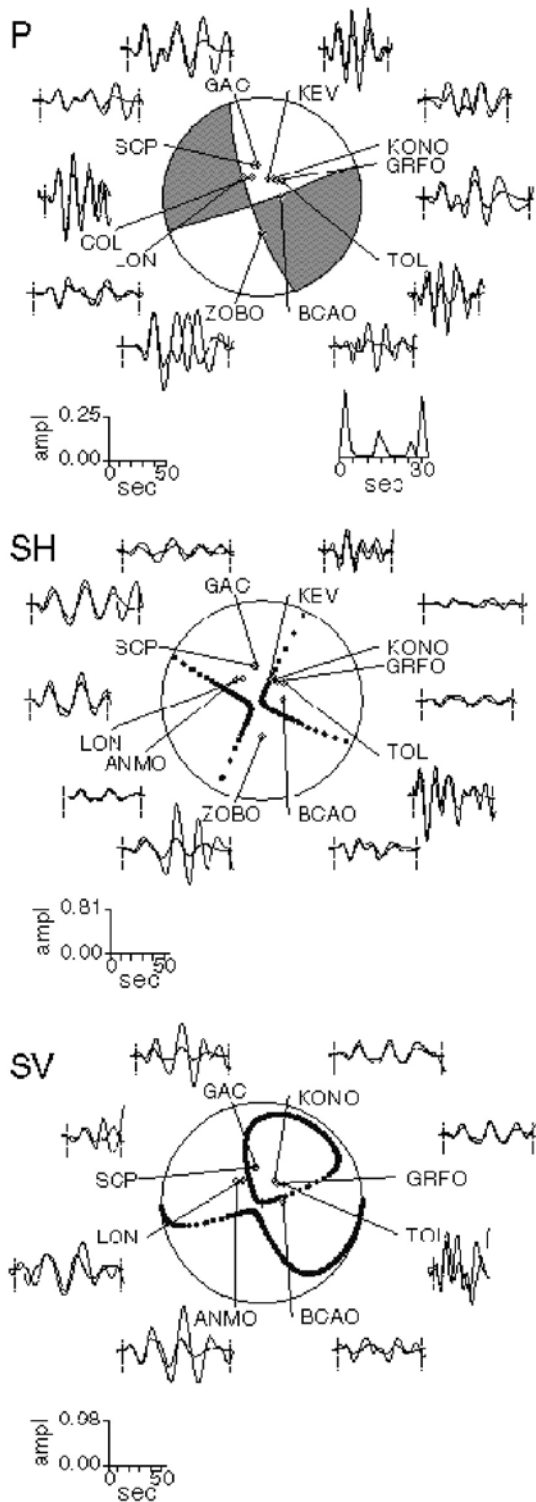


Fig. 4. Comparison between long-period theoretical seismograms (dashed lines) and observed (top) P, (middle) SH, and (bottom) SV waves for the Boca del Tocuyo mainshock, using a point source with a single, long source time function (same focal mechanism for all resulting subevents) with a duration of 30 s. The fit is better than for the shorter source time function (Fig. 3) and shows that at least three point sources are present in the rupture process. Other symbols and amplitude normalization are the same as on Figure 3.

resolved because they contribute most of the moment release on the seismograms (Table 4). The second subevent of the mainshock contributes only 10% of the total moment release and, therefore, the solution is not as well constrained as that of the first and third subevents. Thus we conclude that the mainshock is composed of at least two subevents and possibly a smaller third one triggering between the two larger subevents.

For the largest aftershock, the second subevent occurred 27 s after the first one. The depths of the subevents are 11 km and 12 km respectively and the total seismic moment (tensor sum) of the aftershock is  $2.9 \times 10^{17}$  Nm ( $M_w=5.6$ ). The first subevent of the aftershock has a strike-slip-faulting mechanism similar to the mainshock. The second subevent, however, has a normal-faulting mechanism. The focal mechanism of the second subevent is not well resolved because the wavetrains arrive late and within the coda of the first burst of moment release. Nonetheless, in order to validate the result that the fault plane solution of the second subevent of the aftershock did not correspond to a strike-slip mechanism similar to that of the first subevent, several inversions were carried out fixing the initial parameters of the second subevent with a focal mechanism identical to the first subevent. The results of these inversions showed that the fit between the synthetics and observed seismograms was acceptable for *P*-waves, but not for the *SH*-waves. Furthermore, when the initial parameters of the second subevent were freed, the inversion continuously converged to a normal-faulting fault plane solution.

During the inversion, it was attempted to identify the direction of rupture propagation of the Boca del Tocuyo mainshock, based on a potential correlation with the preferential orientation of the aftershocks and with the strike indicated by the average focal mechanism. This was done by testing whether a directivity pattern was observed in the body waves when the second and third subevents were displaced with respect to the first one. However, no preferred orientation of the rupture could be gleaned from the inversion by allowing the subevents to move relative to one another. The absence of a directivity pattern in the waveforms suggests that the three subevents of the mainshock nucleated very close to one another, probably as a result of episodic slip on the same fault or on neighboring faults.

### Discussion

The analysis of the epicentral locations by the single, and calibration-event methods (Dewey, 1971) using local, regional and teleseismic data suggests that the Boca del Tocuyo earthquakes occurred offshore, very close to the coastal towns exhibiting the most severe and widespread damage. The relocation of the largest aftershock with



Table 4

Source Parameters of the Boca del Tocuyo Earthquakes Determined by the Inversion of Long-Period Body Waves Seismograms

Event	Subevent	Strike deg	Dip deg	Slip deg	Depth km	$M_0$ $10^{18}$ Nm	Delay sec	Duration sec
Apr. 30, 1989	SSTF <sup>1</sup>	162±2	78±1	-178±1	17.0±0.4	1.32±0.06	-	4.00±0.04
	1	162±2	77±1	-179±2	17.5±0.4	1.20±0.06	-	4.00±0.05
	2	159±8	41±4	-161±12	12.5±2.0	0.25±0.04	12.4±0.5	4.00±0.16
	3	164±2	83±1	-174±1	10.8±0.7	0.98±0.06	27.6±0.2	4.00±0.06
	Average <sup>2</sup>	162±1	82±1	-177±1	14.3±0.3	3.5	-	30
May 4, 1989	SSTF1	133±2	83±1	-172±1	10.2±0.7	0.17±0.01	-	4.00±0.04
	1	137±1	76±1	-172±1	11.0±0.5	0.15±0.01	-	4.00±0.03
	2	178±2	56±1	-72±2	12.4±0.6	0.14±0.01	26.9±0.2	4.00±0.04
	Average <sup>2</sup>	130±2	90±2	-172±1	12.0±1.4	0.24	-	30

<sup>1</sup> SSTF: Best double-couple using a short source time function.

<sup>2</sup> Average: Best double-couple of the moment tensor sum of the subevents.

respect to the main event indicates that the aftershock nucleated approximately two km to the NW of the mainshock. Furthermore, the ~60 smaller aftershocks ( $m_b < 4.5$ ) recorded by *FUNVISIS* using a local seismological network were also located at sea, with depths increasing from 0 to 24 km in a NE-SW direction.

The results of the inversion of the bodywaves show that the Boca del Tocuyo earthquakes originated as a result of a multiple rupture process. The complexity of the source caused an anomalously long duration of the body waves of both earthquakes. The duration of the P waves of a simple event of that magnitude is, on average, of about 35 s, whereas in the case of the Boca del Tocuyo mainshock it was of ~75 s. Although no local strong motion data are available, the teleseismic observations suggest that intense shaking took place near the epicentral region for over thirty seconds. This long period of strong shaking was produced by the sequential rupture of the two to three subevents that conform the mainshock, with the second and third subevents triggering about 12 and 28 s after the first one. As discussed above, the inversion of the bodywaves does not allow to accurately measure the spatial relation between the first and the third subevents.

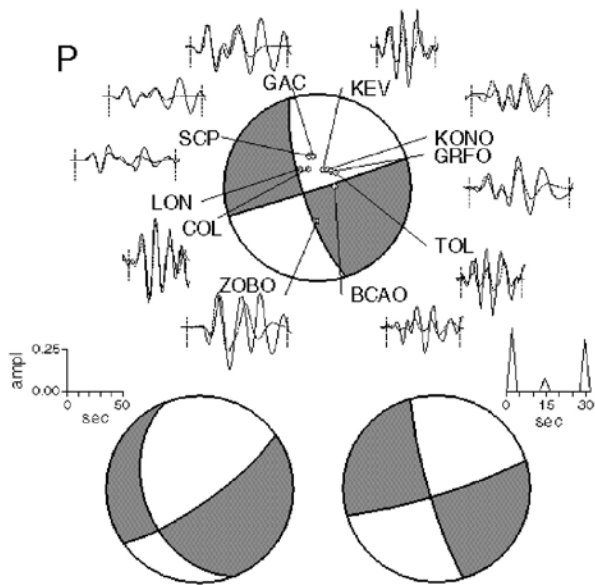
The strike-slip focal mechanisms obtained from the inversion of the Boca del Tocuyo mainshock and its largest aftershock are similar to those reported by Dzierwonski *et al.* (1990). The latter show almost identical directions of strike and slip. The larger dip (18°) of the NW-SE striking nodal plane give the Harvard mechanism a slightly larger normal faulting component. Considering that the Harvard solution

is a long-period inversion of a complex event, we consider that the differences to be small and within the errors of the methodologies involved. The solution from *FUNVISIS* was constructed using only local stations at close distances and with very limited azimuthal coverage. The ISC shows that only nine Venezuelan stations reported the event and all located with a backazimuth from the epicenter of between 97° and 285°. Considering the short distances involved to the stations (less than 450 km), the high take-off angles do not permit the construction of a reliable fault plane solution. We ignore the reasons why the NEIC solution differs so dramatically from our results and those of Harvard.

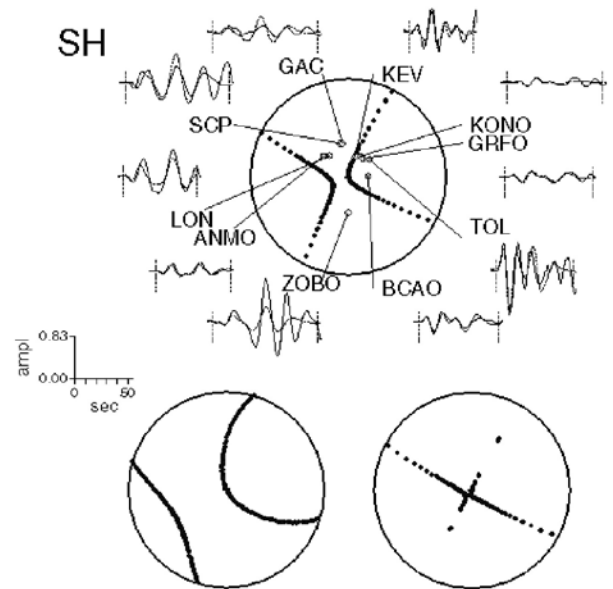
The analysis of which nodal plane of the mechanism corresponds to the ruptured fault is important from a tectonic point of view. As mentioned above, no historical or instrumental earthquakes had been reported in this area before the occurrence of the Boca del Tocuyo seismic sequence. Furthermore, recent studies of the active geological features in this region (Barbot *et al.*, 1979; Barbot *et al.*, 1980; Singer *et al.*, 1992) show evidence of a complex tectonic environment, related to the convergence of the major right-lateral, strike-slip fault systems (Boconó, Oca-Ancón, and Morón) and a set of smaller NW-SE oriented conjugate faults (Figures 1 and 7).

A NW-SE oriented fault plane was selected as the nodal plane of the possible rupture process for the Boca del Tocuyo events based mainly on a report by Singer *et al.* (1992) who suggests a fault plane dipping to the SW. If the fault plane dips to the SW, it would correspond to the NW-SE striking nodal plane of a right-lateral strike-

a)



b)



c)

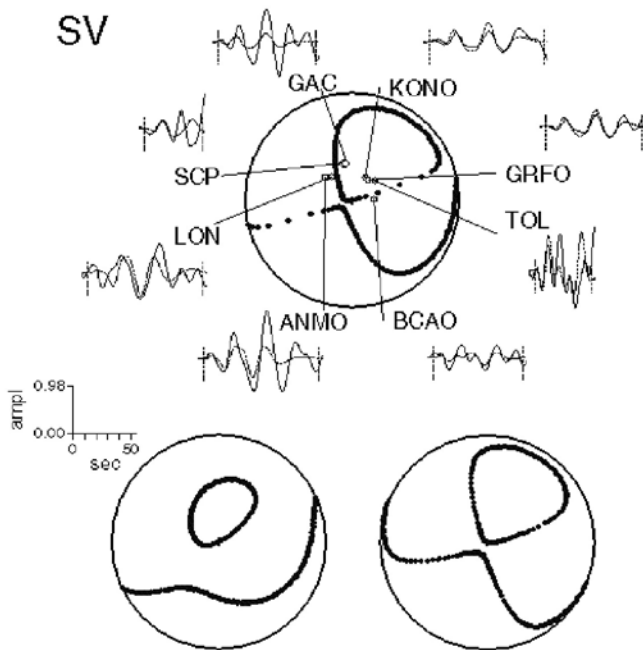


Fig. 5. Results of the simultaneous inversion of the long-period body waves of the Boca del Tucuyo mainshock using three point sources (subevents): a) P waves; b) SH waves; and c) SV waves. The focal mechanism of the first subevent is shown together with the theoretical seismograms (dashed lines) and observed waveforms (solid lines). The fault plane solutions of the second (left) and third (right) subevents are shown at the bottom. The symbols and amplitude normalization are the same as on Figure 3.

slip focal mechanisms gleaned here from the bodywave inversion. Furthermore, this orientation coincides with the orientation of the NW-SE conjugate fault systems mapped offshore that apparently control the shape of the coastline in this region. Several right-lateral, strike-slip faults with a NW-SE orientation have been identified in northwestern Venezuela on both sides of the Peninsula of Paraguaná (Soulas *et al.*, 1987; Singer *et al.*, 1992) (Figure 1). Thus we conclude that the focal mechanism of the Boca del Tocuyo earthquake apparently took place as right-lateral, strike-slip motion on a NW-SE oriented fault. The correlation of the Boca del Tocuyo seismic sequence with a particular fault is not possible.

The occurrence of moderate-sized earthquakes on those conjugate fault systems is important in understanding the tectonic regime in northern Venezuela. As mentioned before, there is an appreciable difference between the rate of motion observed on the Boconó and Oca-Ancón fault systems and that predicted by the relative velocity between

the Caribbean and South American plates. That difference in motion between those plates is possibly being absorbed by slip on these conjugate fault systems, in a complex volumetric deformation.

Earthquakes with multiple rupture processes seem to be a relatively common occurrence in this complex tectonic environment of northern and western Venezuela. In addition to the earthquakes of Boca del Tocuyo, two more examples of multiple source events have been suggested: the great earthquake of March 26, 1812, and the Caracas earthquake of 1967. On the basis of damage reports, the earthquake of 1812 has been interpreted as consisting of at least two distinct events (Kelleher *et al.*, 1973). On the other hand, the Caracas earthquake of 1967 has been interpreted as the sum of at least three subevents (Rial, 1978; Suárez and Nábelek, 1990). These earthquakes reflect the presence of a complicated regional pattern associated with a wide deformation zone along the Caribbean-South America border.

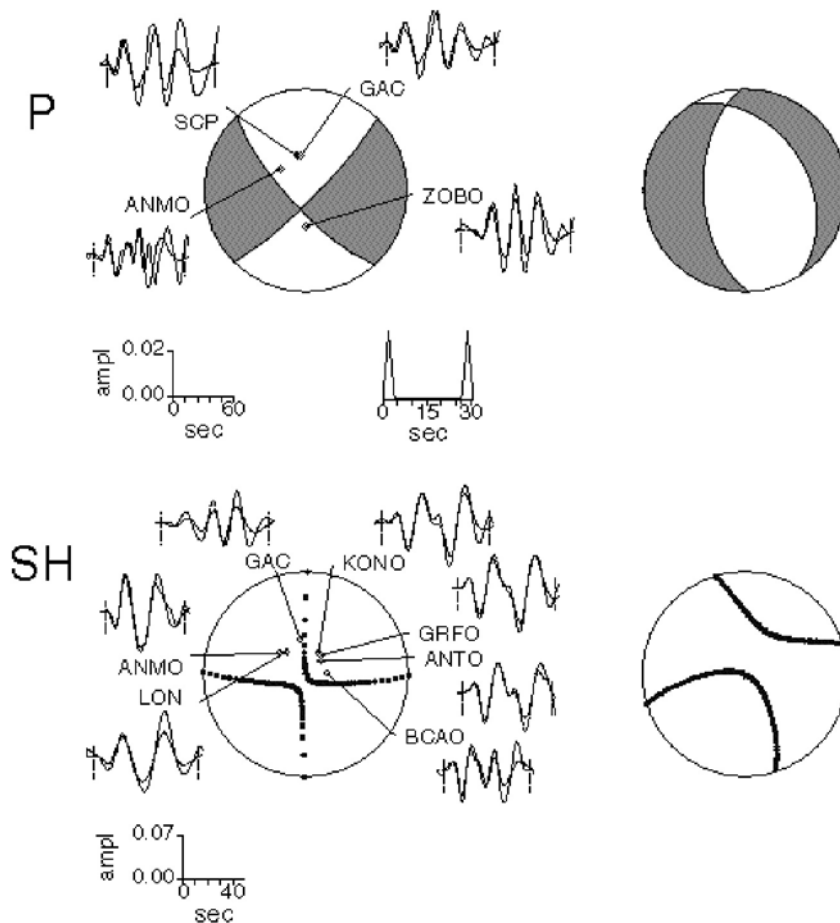


Fig. 6. Results of the simultaneous inversion of the long-period body waves P and SH for the Boca del Tocuyo aftershock using two point sources (subevents). The focal mechanism of the first subevent is shown together with the theoretical seismograms (dashed lines) and observed waveforms (solid lines). The fault plane solution of the second subevent is shown to the right of the first one. Other symbols and amplitude normalization are the same as for Figure 3.

The liquefaction induced by the Boca del Tocuyo earthquakes appears to be more intense and widespread than expected for an earthquake of that magnitude. Liquefaction occurs in soils when the pore-water pressure builds up under ground shaking and equals the confining pressure of the saturated and unconsolidated deposits. This produces a loss of the shear strength of the soil (e.g., Ambraseys and Sarma, 1969). This increase of pore pressure may be originated either by a rapid pulse of high stress or by a long train of comparatively weak pulses. In the latter case, liquefaction depends on the continuity and duration of the seismic excitation, both of which allow the pore-water pressure to build up gradually.

One may speculate that the intensity and extent of the observed liquefaction induced by the Boca del Tocuyo events occurred mainly as a result of the local soil conditions, but that it was perhaps enhanced by the long and sustained levels of intense shaking produced by the complex and long rupture process. Furthermore, the sequential initiation and stopping of the rupture process induced by this complex source, probably resulted in anomalously

rich high-frequency waveforms. Unfortunately, no local recordings exist to confirm this hypothesis. It should be noted that the effect of initiation and stopping phases of a multiple rupture process would be independent to the relative location of the subevents composing the main rupture process.

In contrast, on July 12, 1988, a shallow event of magnitude  $m_b=5.4$  occurred beneath Lake Maracaibo, in western Venezuela, in close proximity to several places where soil conditions are very similar to those in Boca del Tocuyo. This event, however, did not produce liquefaction. The reason is perhaps that the 1988 Lake Maracaibo earthquake was a simple event (Malavé, 1992; Malavé and Suárez, 1993), whereas the Boca del Tocuyo earthquakes exhibited an anomalously long duration of the body-wave trains.

### Summary and Conclusions

The Boca del Tocuyo earthquake of 1989 ( $m_b=5.7$ ) is one of the largest instrumentally recorded events in western

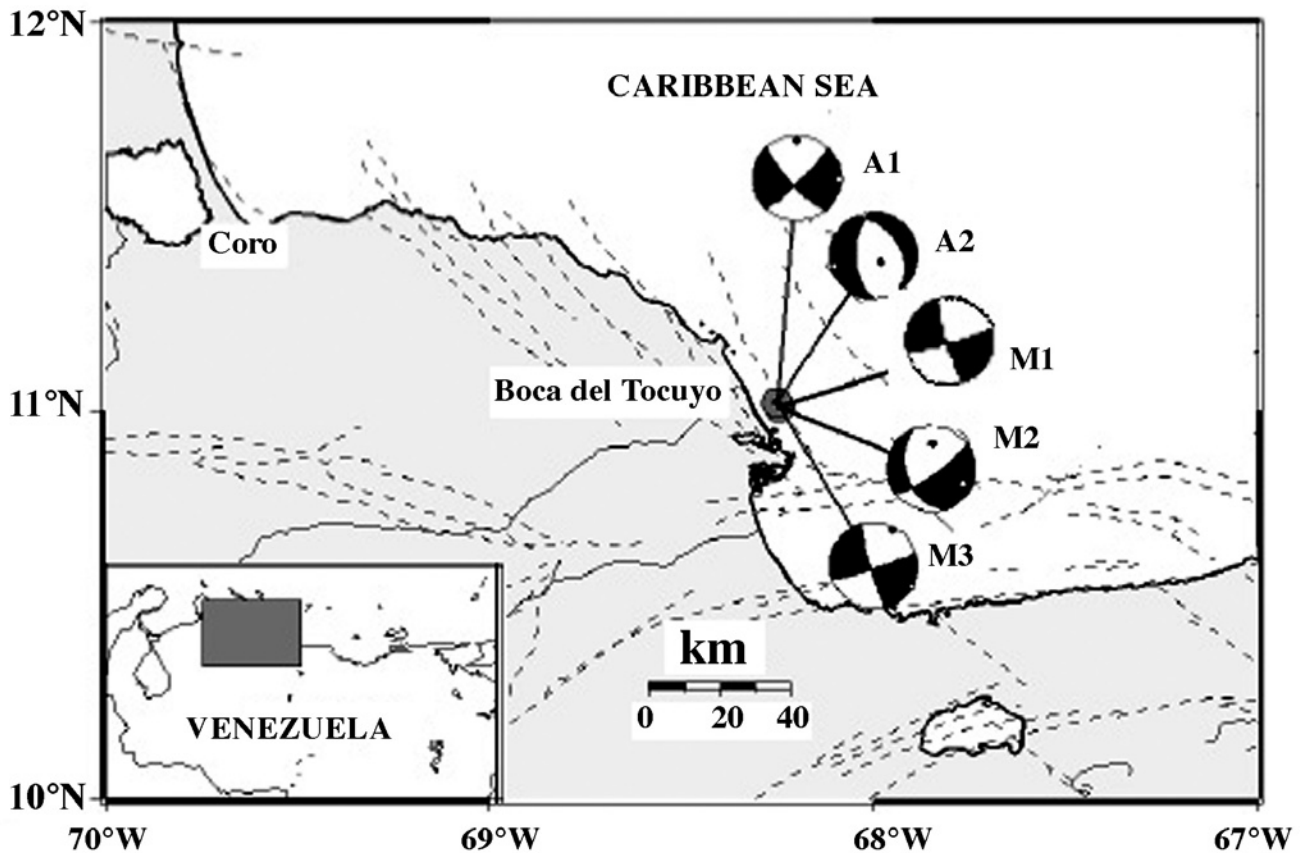


Fig. 7. Summary of the focal mechanisms obtained from the body wave inversion of the Boca del Tocuyo mainshock and its largest aftershock. M1, M2 and M3 represent the focal mechanisms of the three subevents composing the mainshock and A1 and A2 are the mechanisms of the two subevents that generated the largest aftershock. Symbols as in previous figures.

Venezuela. Both historical and instrumental records show a dearth of earthquakes in this coastal area before the seismic sequence of April and May, 1989. The inversion of the *P*, *SH*, and *SV* waves indicates that the source time function of the main earthquake is composed of at least two and perhaps three subevents, distributed over a time span of 30 s. The focal mechanisms of the three subevents of the mainshock show right-lateral, strike-slip faulting at an average depth of 14 km. The focal mechanism of the largest aftershock is composed of two subevents, the first subevent of the aftershock indicates strike-slip faulting similar to the fault plane solution of the mainshock. However, the focal mechanism of the second subevent shows tensional dip-slip faulting.

It was not possible to unequivocally identify the direction of rupture propagation using the inversion algorithm. However, one of the fault planes is oriented in NW-SE direction with right-lateral, strike-slip displacement. This orientation coincides with the direction of a fault system which is conjugate to the east-west major fault systems that have been postulated as the current boundary between Caribbean and South American plates.

One may speculate that the intense liquefaction caused by these two earthquakes appears to be a consequence of the presence of water saturated, unconsolidated sediments, enhanced by the long and sustained duration of strong ground shaking induced by the multiple rupture process. Also, the resulting seismic waves near the epicentral area were probably rich in high-frequency content due to the complexity of the source time function.

#### Acknowledgments

The authors thank A. Espinosa, C. Mendoza, S. K. Singh for their thoughtful reviews of the manuscript. Two anonymous reviewers gave us valuable comments that substantially improved the manuscript. M. Zirbes made available copies of the *GDSN* seismograms and J. W. Dewey gave us a copy of his *JHD* computer programs. We also want to thank the staff of *FUNVISIS* for the information provided and helpful suggestions. This work was finished while one of the authors (*GM*) was a graduate student at the Universidad Nacional Autónoma de México under a fellowship from INTEVEP, S.A. This work was finished when one of us (*GS*) was a visiting professor at the Istituto Nazionale di Geofisica, Milano. Thanks are due to M. Stucchi for his generous support.

#### Bibliography

AMBRASEYS, N. and S. SARMA, 1969. Liquefaction of soils induced by earthquakes. *Bull. Seism. Soc. Am.* 59 (2), 651-664.

AMBRASEYS, N., 1988. Engineering Seismology. *Int. J. Earthquake Eng. Struct. Dyn.* 17, 1-105.

AUDEMARD, F. and F. DE SANTIS, 1991. Prospect-pit survey of liquefaction structures induced by recent moderate earthquakes. *Bull. Int. Assoc. Eng. Geol.* 44, 5-16.

BARBOT, J. P., J. BUTENKO and J. I. RODRÍGUEZ, 1979. Geologic and geotechnical analysis of Golfo Triste: its influence on offshore structures and drilling operations, Congress COPPE/UFRJ, Rio de Janeiro, 17 pp.

BARBOT, J. P., J. BUTENKO, E. ESPINOZA, J. DAZA, and G. MALAVÉ, 1980. El cuaternario del Golfo de La Vela y su importancia geotécnica para la exploración y explotación petrolera, Transactions 9th Caribbean Geological Conference, Santo Domingo, 2, 541-553.

BOYD, T. and J. NÁBĚLEK, 1988. Rupture process of the Andean Islands earthquake of May 7, 1986. *Bull. Seism. Soc. Am.* 78 (5), 1653-1673.

BYRNE, D., L. SYKES and D. DAVIS, 1992. Great Thrust Earthquakes and Aseismic Slip Along the Plate Boundary of the Makran Subduction Zone. *J. Geophys. Res.* 97 (B1), 449-478.

DE SANTIS, F., C. BELTRÁN, F. AUDEMARD, A. FERNÁNDEZ, A. SINGER, A. ADRIANZA, L. MONTES, M. LUGO and C. CHACÍN, 1991. Estudio de las manifestaciones de licuefacción de suelo ocurridas en Falcón Oriental durante los sismos de abril y mayo de 1989: aspectos geológicos y geotécnicos, *FUNVISIS*, Caracas, Venezuela.

DEWEY, J. W., 1971. Seismic studies with the method of Joint Hypocenter Determination, Ph.D. Thesis, Univ. of Calif., Berkeley, 164 pp.

DZIEWONSKI, A. M., G. EKSTROM, J. H. WOODHOUSE, and G. ZWART, 1990. Centroid-moment tensor solutions for April-June 1989. *Phys. Earth Planet. Int.* 60, 243-253.

GAJARDO, E., J. L. NICOLLE, B. CASTEJÓN, C. MÁRQUEZ, and M. URBÁEZ, 1986. Modelo de corteza de la Costa Oriental del Lago de Maracaibo, III Congreso Venezolano de Geofísica, Caracas, Venezuela, 102-111.

HANKS, T. and H. KANAMORI, 1979. A moment magnitude scale. *J. Geophys. Res.* 84, 2348-2350.

- HERRIN, E., E. P. ARNOLD, B. A. BOLT, G. E. CLAWSON, E. R. ENGDahl, H. W. FREEDMAN, D. W. GORDON, A. L. HALES, J. L. LOBDELL, O. NUTTLI, C. ROMNEY, J. TAGGART and W. TUCKER, 1968. 1968 seismological tables for P phases. *Bull. Seismol. Soc. Am.* 58, 1196-1241.
- JORDAN, T. H., 1975. The present-day motions of the Caribbean plate. *J. Geophys. Res.* 80, 4433-4439.
- KAFKA, A. and D. WEIDNER, 1981. Earthquake focal mechanisms and tectonic processes along the southern boundary of the Caribbean plate. *J. Geophys. Res.* 86 (B4), 2877-2888.
- KELLEHER, J., L. R. SYKES and J. OLIVER, 1973. Possible criteria for predicting earthquake locations and their application to major plate boundaries of the Pacific and the Caribbean. *J. Geophys. Res.* 78, 2547-2585.
- MALAVÉ, G., 1992. Inversión de ondas de volumen de algunos sismos importantes del noroccidente de Venezuela: relación con la tectónica regional, M.Sc. Thesis, Universidad Nacional Autónoma de México, México D.F., México, 93 pp.
- MALAVÉ, G. and G. SUÁREZ, 1993. Recent seismicity ( $m_b \geq 5.4$ ) in western Venezuela: regional tectonic implications, Second International Symposium on Andean Geodynamics, Oxford, England, 111-114.
- MALAVÉ, A., 1990. El sismo de Boca del Tocuyo del 30 de abril de 1989, Memorias de las Segundas Jornadas de Ingeniería Sísmica, Caracas, Venezuela.
- MINSTER, J. B. and T. H. JORDAN, 1978. Present-day plate motions. *J. Geophys. Res.* 83, 5331-5334.
- MOLNAR, P. and L. SYKES, 1969. Tectonics of the Caribbean and Middle America Regions from Focal Mechanisms and Seismicity. *Geol. Soc. Am. Bull.*, 80, 1639-1684.
- NÁBELEK, J. L., 1984. Determination of earthquakes source parameters from inversion of body waves, Ph.D. Thesis, Massachusetts Institute of Technology, Cambridge, 361 pp.
- RIAL, J. A., 1982. The Caracas, Venezuela, earthquake of July 1967; a multiple source event. *J. Geophys. Res.* 83, 5405-5415.
- SCHUBERT, C., 1982. Neotectonics of Boconó fault, western Venezuela. *Tectonophysics* 85, 205-220.
- SINGER, A., F. AUDEMARD, C. BELTRÁN, J. A. RODRÍGUEZ, F. DE SANTIS, A. ADRIANZA, C. CHACÍN, M. LUGO, J. MENDOZA and C. RAMOS, 1992. Actividad tectónica cuaternaria y características sísmogénicas de los sistemas de fallas de Oca-Ancón (tramo oriental), de la península de Paraguaná y región de Coro y de la costa nororiental de Falcón, FUNVISIS, Caracas, Venezuela.
- SIPKIN, S. and R. NEEDHAM, 1991. Moment tensor solutions estimated using optimal filter theory: global seismicity, 1988-1989. *Phys. Earth Planet. Int.* 67, 221-230.
- SOULAS, J. P., 1986. Neotectónica y tectónica activa en Venezuela y regiones vecinas, Memorias VI Congreso Geológico Venezolano X, Caracas, Venezuela, 6639-6656.
- SOULAS, J. P., C. GIRALDO, D. BONNOT and M. LUGO, 1987. Actividad cuaternaria y características sísmogénicas del sistema de fallas Oca-Ancón y de las fallas de Lagarto, Urumaco, Río Seco y Pedregal. Afinamiento de las características sísmogénicas de las fallas de Mene Grande y Valera, FUNVISIS, Caracas, Venezuela.
- STEIN, S., C. DEMETS, R. G. GORDON, J. BRODHOLT, D. ARGUS, J. F. ENGELN, P. LUNGREN, C. STEIN, D. A. WIENS and D. F. WOODS, 1988. A test of alternative Caribbean plate relative motion models. *J. Geophys. Res.* 93, 3041-3050.
- SUÁREZ, G. and J. NÁBELEK, 1990. The 1967 Caracas Earthquake: Fault Geometry, Direction of Rupture Propagation and Seismotectonic Implications. *J. Geophys. Res.* 70, 5065-5074.
- SYKES, L., W. R. MCCANN, and A. L. KAFKA, 1982. Motion of Caribbean plate during last 7 million years and implications for earlier Cenozoic movements. *J. Geophys. Res.* 87, 10656-10676.

Gustavo Malavé<sup>1</sup> and G. Suárez<sup>2,\*</sup>

<sup>1</sup> Fundación Venezolana de Investigaciones Sismológicas (FUNVISIS), Av. Guaicaipuro con calle Tiuna, El Llanito, 1070 Caracas, Venezuela

Email: gmalave@funvisis.gob.ve

<sup>2</sup> Instituto de Geofísica, Universidad Nacional Autónoma de México, Del. Coyoacán 04510 Mexico City, México.

\*Corresponding author: gerardo@ollin.igeofcu.unam.mx